Regular Article

Evaluation of the Theranostic Potential of Perfluorohexane-Based Acoustic Nanodroplets

Rodi Abdalkader,[a] Johan Unga,[c] Fumiyoshi Yamashita,[b] Kazuo Maruyama,[c] and Mitsuru Hashida*,[a]

[a] *Institute for Advanced Study (KUIAS), Institute for Integrated Cell-Material Sciences (iCeMS), Kyoto University; Yoshida Ushinomiya, Sakyo-ku, Kyoto 606–8501, Japan:* [b] *Graduate School of Pharmaceutical Sciences, Kyoto University; 46–29 Yoshida-Shimo-Adachi, Sakyo-ku, Kyoto 606–8501, Japan: and* [c] *Faculty of Pharma-Sciences, Teikyo University; 2–11–1 Kaga, Itabashi-ku, Tokyo 173–8605, Japan.*

Received June 24, 2019; accepted September 12, 2019; advance publication released online September 25, 2019

In this study, we have prepared perfluorohexane (PFH)-based acoustic nanodroplets (PFH-NDs) and evaluated their theranostic characteristics. Nile Red (NR) was incorporated into PFH-NDs as a model of hydrophobic drugs (NR-PFH-NDs). The mean particle diameters of PFH-NDs and NR-PFH-NDs were 205 ± 1.8 nm and 346.3 ± 6 nm, respectively. There was no significant PFH leakage from PFH-NDs during 90 min incubation at 37°C in the presence of 10% rat serum. The *in vitro* ultrasonography showed that the phase transition of PFH-NDs from liquid droplets to gassed bubbles could be induced by therapeutic low-intensity ultrasound with a frequency of 1 MHz and an intensity of 5 W/cm^2. Irradiation of ultrasound in combination with NR-PFH-NDs enhanced uptake of NR in murine adenocarcinoma cells (C26). After intravenous injection of PFH-NDs to mice, PFH gradually disappeared from blood circulation with an elimination half-life of 43.3 min. Intravenous injection of PFH-NDs also resulted in significant contrast enhancement in the mouse carotid artery upon therapeutic low-intensity ultrasound irradiation. These results suggest the potential of PFH-NDs as a novel contrast agent for further theranostic applications.

Key words nanodroplet; perfluorohexane; ultrasound; phase-transition; theranostics

INTRODUCTION

Theranostics is a term that refers to the combination of therapy and diagnostics so that for instance the same nanoparticle can both be applied for finding a disease location and delivering drugs for treatment with this concept. Ultrasonography is a well-known and safe diagnostic tool, while its limitation is with the difficulty in recognising the blood vasculature from the surrounded tissues, and therefore ultrasound contrast agents (UCAs) such as microbubbles (MBs) are commonly used for intensifying the contrast signal in the blood vasculature.[1–3] In MBs, hydrophobic gases such as perfluorocarbons (PFCs) are stabilized in bubble form with biocompatible shells. Consequently, MBs are mostly as large as 0.5–2 μm in diameter.[3–5] MBs-mediated sonoporation is also reported to be useful for *in vivo* delivery of anti-cancer agents and plasmid DNA.[3,6–8] Because of their large sizes, however, MBs are rapidly sequestered from the blood circulation: Toft *et al.* estimated a blood elimination half-life of perfluorobutane gas MBs shelled with hydrogenated egg phosphatidylserine (Sonazoid®) to be 2–3 min in rats.[9] Our results for doxorubicin-loaded MBs with a phospholipid shell and perfluoropropane gas core gave a similar elimination half-life of 2–3 min in mice.[3] Instability of MBs in the circulation is due to the exchange of the fluorocarbon gas core with gases dissolved in the blood such as oxygen, nitrogen and carbon dioxides.[10] MBs precursors known as phase shift acoustic nanodroplets should be a possible solution for improving the stability of microbubbles and then their theranostic features.[11] Liquid PFCs with a high boiling point are stable at the room temperature and can form nanodroplets (NDs) by emulsifying with surface active biocompatible molecules such as phospholipids. Droplets structure entails a monolayer of phospholipids or surfactants that pack liquid PFCs in the droplet's cores. The thermal or acoustic pressure effect of therapeutic ultrasound triggers droplets imposing a phase transition from liquid to gas and generating bubbles.[12] Compared to polymer-based NDs, phospholipid-based NDs have better resonant properties due to the high elasticity of the phospholipid shells.[13] So far, many phospholipid-based NDs have been examined; mainly for their potential in ultrasonography.[14–16] Their potential use in cancer therapy has also been demonstrated in several reports.[17–19] In these studies, liquid perfluoropentane (PFPn) and perfluorohexane (PFH) have been two popular PFCs materials for NDs, while PFH can be superior to PFPn regarding favourable durability against repeated therapeutic ultrasound activation due to its high boiling point.[20] That means NDs with the PFH core are re-condensed from the evaporated state more easily. Theranostic NDs needs to obtain several characteristics such as high contrast signal, sufficient drug payload, and most importantly the stability under *in vivo* conditions, those ensure the theranostic functions. Therefore, the high *in vivo* durability and the long-lasting contrast signal of PFH-NDs are expected to improve the theranostic characteristics of UCAs. In the present study, we evaluated the theranostic features of PFH-NDs including their *in vitro* and *in vivo* functions in mice.

MATERIALS AND METHODS

Materials 1,2-Distearoyl-*sn*-glycero-3-phosphocholine (DSPC) and 1,2-distearoyl-*sn*-glycero-3-phosphatidylethanol-

* To whom correspondence should be addressed. e-mail: hashidam@pharm.kyoto-u.ac.jp

amine *s*-methoxypolyethyleneglycol (PEG_{2000}-DSPE, (PEG, M_w = approx. 2000)) were purchased from Avanti Polar Lipid Inc. (Alabaster, AL, U.S.A.) and NOF Co. (Tokyo, Japan), respectively. PFH and Nile Red (NR) were obtained from Sigma-Aldrich (St. Louis, MO, U.S.A.).

Cells and Animals The murine colon adenocarcinoma cell line (C26) was obtained from the American Type Culture Collection (ATCC, Manassas, VA, U.S.A.). Cells were cultured at 37°C with 5% CO_2 in Dulbecco's modified Eagle's medium obtained from Nissui Pharmaceutical Co., Ltd. (Tokyo, Japan) supplemented with 10% fetal bovine serum and 100 U/mL penicillin/streptomycin.

Female 6-week-old ICR mice and 6-weeks female wistar rats were purchased from the Shizuoka Agricultural Cooperation Association for Laboratory Animals (Shizuoka, Japan). All experiments were approved by the Animal Experimentation Committee of the Graduate School of Pharmaceutical Sciences, Kyoto University and by Teikyo University School of Medicine Animal Ethics Committee number 14-027.

Preparation of NDs Preparation of of NDs was carried out with two steps. First, phospholipid vesicles (liposomes) were prepared with DSPC and PEG_{2000}-DSPE at 94 : 6 M ratio. Lipids were dissolved in chloroform and transferred to a round-bottom flask. Following evaporation of the solvent under reduced pressure, the formed lipid thin film was thoroughly dried under vacuum overnight. The obtained lipid thin film was hydrated with phosphate-buffered saline (PBS) solution (8 mg Lipid/mL) at 65°C for 60 min under mild shaking, exposed to bath-type sonication for 3 min, and then exposed to tip sonication for 2 min. In the second step for preparing NDs, 1 mL of the liposome solution was transferred to a 2 mL sterilized vial, followed by adding 60 μL PFH (Sigma-Aldrich) to end up with 6% (v/v) of PFH suspension. In preparation of NR-PFH-NDs, NR was dissolved to PFH-NDs at a concentration of 375 μg/mL as a model drug in the vial. The vial was then capped and exposed to bath type sonication for 3–5 min on ice. All sample formulations were kept at 4°C until further use.

The Characterization of Particle Size and Stability of PFH-NDs The particle size of the liposomes and NDs were determined using Zetasizer Nano instrument (Malvern Instruments, Worcestershire, U.K.). *In vitro* stability of PFH-NDs in the presence of serum was evaluated by determining the remaining amount of PFH in PFH-NDs sample during incubation. Briefly, 100 μL PFH-NDs were mixed with 500 μL PBS containing 10% of rat serum obtained from female wistar rats and incubated in a water bath at 37°C. Ten microliters samples were collected at different time points and analyzed with GC-MS under conditions described in the previous report.[21] The retention percentage of PFH was obtained by normalizing the peak area of PFH at specific time to the peak area of PFH at zero time.

***In Vitro* Echogenicity of PFH-NDs** A rubber tube was placed in a water bath kept at 37°C. One and half milliliters of degassed distilled water was filled in the tube and then left for 10 min for temperature equilibrium. A diagnostic ultrasound transducer was fixed at the edge of the rubber tube and then three echo images were taken as a background signal using an ultrasonography system (Vevo 2100, FUJIFILM VisualSonics, Toronto, Canada). After that, 10 μL of PFH-NDs solution was added and mixed well with a pipette. An external ultrasound transducer was immersed in the rubber tube in a way so that it did not interfere with the ultrasonography probe. Each sample solution was irradiated with ultrasound at different frequencies, intensities, and exposure times followed by taking another three images. Ultrasound signal enhancement was evaluated and the difference between before and after ultrasound irradiation was calculated. The mechanical index (MI) value was calculated from the modified equations:

$$MI = \frac{P}{\sqrt{f}} \tag{1}$$

$$P = \frac{force}{unite} \tag{2}$$

$$P = I \tag{3}$$

Where P is ultrasound negative peak pressure, f is the ultrasound frequency, and I is the ultrasound intensity. P was theoretically considered equivalent to I.

***In Vitro* Nile Red Uptake by C26 Cells** C26 cells were seeded in the density of 3×10^4 per well in 8-well glass chamber slide for overnight and NR-PFH-NDs (80 μg of lipid) were added to the culture medium. Three minutes later, ultrasound irradiation was applied in intensity of 5 w/cm^2 and frequency of 1 or 2 MHz for 30 s. Cells were then incubated for 20 min, washed with PBS two times, and then fixed with 4% paraformaldehyde for 10 min at room temperature. NR localization in cells was detected by the fluorescence microscopy (BZ-8100, Keyence, Osaka, Japan).

***In Vivo* Blood Elimination of PFH after Intravenous Injection of PFH-NDs in Mice** PFH-NDs injection sample containing 1.3% (v/v) PFH and 360 μg lipids in a final volume of 200 μL in PBS solution was intravenously injected *via* the tail vein of mice. After 3, 30, 60, and 180 min, mice were sacrificed, and blood samples were obtained. Samples were moved into gas-chromatography vials, capped, and kept at 4°C until GC-MS analysis. The amount of PFH associated with blood was quantified by GC-MS, and the peak area of PFH was normalized by a millilitre of blood volume. Non-compartmental pharmacokinetic analysis was performed as follow: The elimination constant (K) was estimated by plotting the time scale against the logarithmic scale of PFH and the elimination half-life ($t_{1/2}$) was calculated as 0.693 divided by K.

***In Vivo* Ultrasonography Imaging** A dose of PFH-NDs containing 0.7% (v/v) PFH and 225 μg lipids was injected intravenously to mice *via* the tail vein in a final volume of 200 μL. Two minutes post injection, 1000 frames of ultrasonography video were recorded with the Vevo 2100 system. Upon confirming its location in advance with the Doppler mode, the region around the left carotid was imaged. During the monitoring period, two shots of ultrasound irradiation (at Frames 568 and 783) were applied to provoke phase transition of the droplets into bubbles. The images were shown in linear mode and the contrast enhancement.

Statistical Analysis All data were analyzed as mean ± standard error of the mean (S.E.M.). The Dunnett's multiple comparison test was applied using GraphPad prism software.

RESULTS

The Characterization of PFH-NDs

The Particle Size of PFH-NDs

Liposomes employed for the preparation of PFH-NDs had an average particle size of 101 ± 1.0 nm. On the other hand, the PFH-NDs had an average size of 205 ± 1.8 nm, while NR-PFH-NDs had an average size of 346 ± 6 nm (Table 1).

In Vitro Stability of PFH-NDs in the Presence of Rat Serum Determined by PFH Leakage

Samples of PFH-NDs were incubated in the presence of serum for 120 min at 37°C, and the amount of PFH remaining in the sample was determined by GC-MS. The level of PFH remained highly trapped in NDs for 90 min, but after 120 min,

Table 1. Mean Particle Size of Liposomes and PFH Nanodroplets

Formulation	Composition	Particle size (nm)[a)]
Liposome	DSPC/PEG_{2000}-DSPE	101 ± 1.0
PFH-NDs	DSPC/PEG_{2000}-DSPE/C_6F_{14}	205 ± 1.8
NR-PFH-NDs	NR/DSPC/PEG_{2000}-DSPE/C_6F_{14}	346 ± 6.0

a) Data are shown as mean ± S.E.M. ($n = 3$).

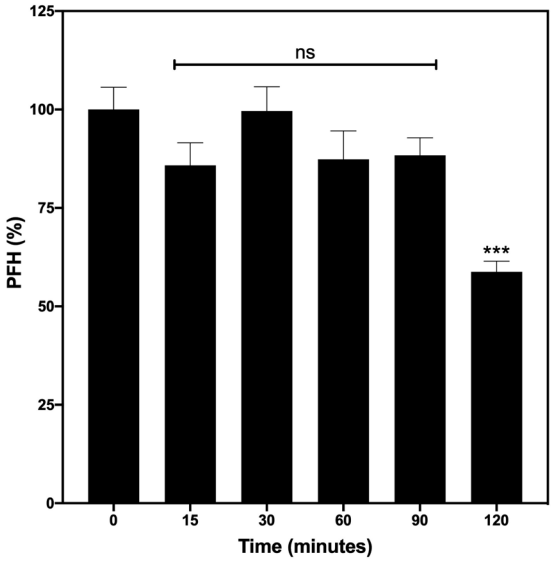

Fig. 1. PFH Leakage *in Vitro* in the Presence of Rat Serum

PFH-NDs were incubated in 10% rat serum in PBS^- at 37°C, and at specific time points, samples were collected for GC-MS analysis of PFH. ($n = 3$; mean ± S.E.M.). ***$p < 0.001$, ns (not significant) *versus* PFH % at 0 time.

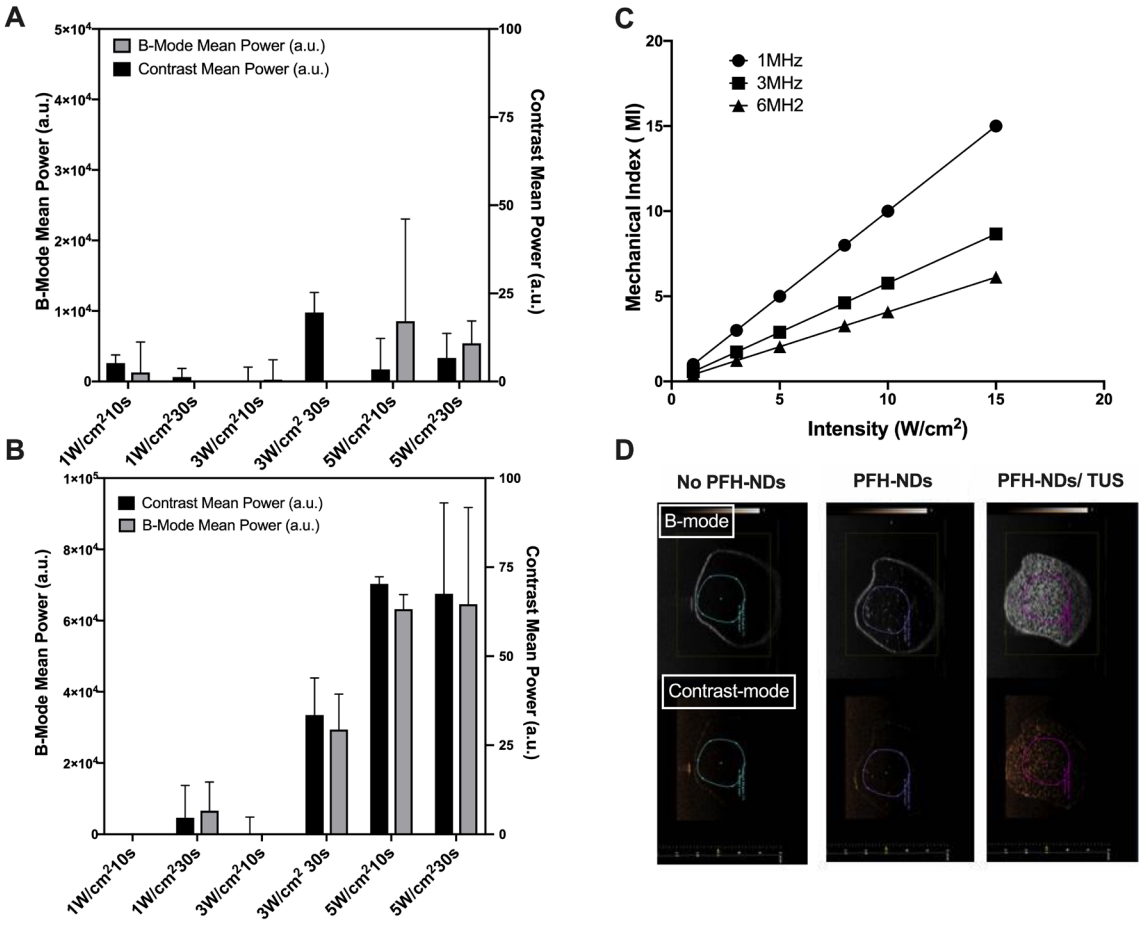

Fig. 2. *In Vitro* Ultrasonography Imaging of PFH-NDs

(A) PFH-NDs activation by therapeutic ultrasound irradiation with a frequency of 3 MHz and different intensities and irradiation times. (B) PFH-NDs activation by ultrasound with a frequency of 1 MHz and different intensities and irradiation times. (C) The effect of ultrasound frequency and intensity on the mechanical index (MI). (D) Ultrasound images of PFH-NDs activation by TUS in the frequency of 1 MHz and fixed intensity of 5 W/cm^2. Images are shown in both brightness mode (upper) and contrast mode (lower). A diagnostic ultrasound transducer was fixed at the edge of the rubber tube and then three echo images were taken as a background signal using an ultrasonography system. After that, PFH-NDs solution was added. An external ultrasound transducer was immersed in the rubber tube. Each sample solution was irradiated with ultrasound at different frequencies, intensities, and exposure times followed by taking another three images. ($n = 3$; mean ± S.E.M.). (Color figure can be accessed in the online version.)

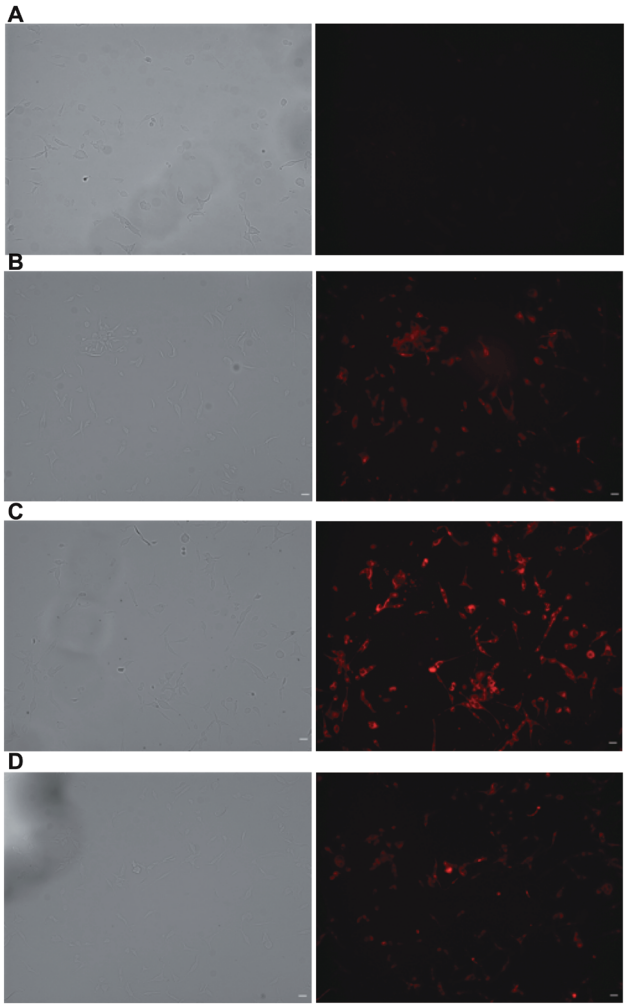

Fig. 3. *In Vitro* NR Uptake in C26 Cells after the Exposure to Ultrasound Irradiation

(A) No treatment; neither with NR-PFH-NDs nor with ultrasound irradiation. (B) NR-PFH-NDs only. (C) NR-PFH-NDs in combination with ultrasound irradiation in the frequency of 1 MHz. (D) NR-PFH-NDs in combination with ultrasound irradiation in the frequency of 2 MHz. Cells were treated with NR-PFH-NDs followed by the exposure to ultrasound irradiation in intensity of 5 w/cm^2 and frequency of 1 or 2 MHz for 30 s. Cells were then incubated for 20 min, washed with PBS two times, and then fixed with 4% paraformaldehyde for 10 min at room temperature. NR localization was detected by the fluorescence microscopy (Scale bars, 20 μm).

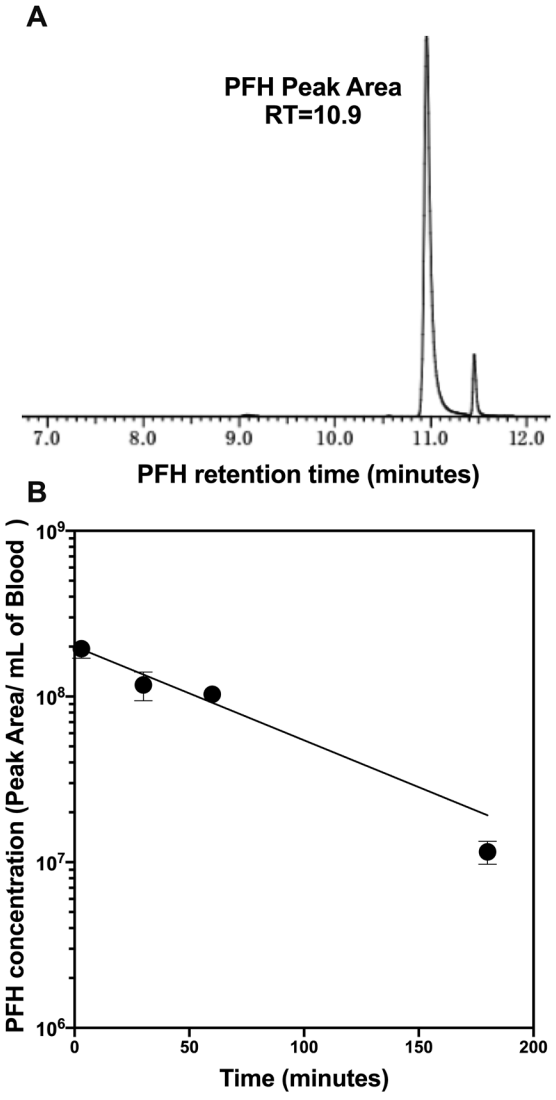

Fig. 4. *In Vivo* PFH Retention in the Blood Circulation of Mice

(A) The detection of PFH peak area at a retention time of 10.9 min in GC-MS analysis. (B) The time–course of PFH concentration in blood during 180 min. Mice were intravenously injected with PFH-NDs, and at 3, 30, 60, and 180 min after injection, blood samples were collected. Samples were moved into gas-chromatography vials, capped, and kept at 4°C until GC-MS analysis. The amount of PFH associated with blood was quantified by GC-MS, and the peak area of PFH was normalized by a millilitre of blood volume ($n = 3$–5; mean ± S.E.M.).

41.2% of PFH was leaked (Fig. 1).

***In Vitro* Echogenicity of PFH-NDs** Effects of ultrasound frequency, intensity, and duration on the phase transition of the PFH-NDs to bubbles were investigated *in vitro* using ultrasonography. At the frequency of 1 MHz, a notable phase shift occurred; represented in the increase of the contrast signal. The maximum contrast enhancement was achieved with ultrasound intensity of 5 W/cm^2 (Figs. 2B, 2D). When PFH-NDs were irradiated with a frequency of 3 MHz, on the other hand, no contrast enhancement was observed even at the highest intensity (Fig. 2A). Thus, ultrasound frequency was appeared to be a critical parameter for the phase shift of the PFH-NDs. The theoretical simulation of the relationship among ultrasound irradiation intensity, frequency, and mechanical index indicated that ultrasound of 1 MHz increased the mechanical index dramatically compared with higher frequency values (Fig. 2C).

***In Vitro* NR Uptake by C26 Cells** Potential of NR-PFH-NDs in NR delivery was evaluated in C26 cells using the fluorescence microscopy. The combination of NR-PFH-NDs with ultrasound irradiation in the frequency of 1 MHz and intensity of 5 w/cm^2 led to a notable cellular accumulation of NR after 20 min of treatment as compared with NR-PFH-NDs in the absence of ultrasound irradiation (Figs. 3B, 3C). Interestingly, the combination of NR-PFH-NDs with ultrasound irradiation in the frequency of 2 MHz and intensity of 5 w/cm^2 did not cause any significant localization of NR (Fig. 3D).

PFH Retention in the Blood Circulation of Mice Mice were intravenously injected with a single dose of PFH-NDs, and PFH levels in blood were periodically quantified by GC-MS. From the time–course of blood PFH levels, the elimination constant (K) of 0.016 min^{-1} and elimination half-life ($T_{1/2}$) of 43.3 min for PFH were obtained (Fig. 4).

***In Vivo* Ultrasonography Imaging** The location of the left carotid artery was confirmed in advance by using colour Doppler mode and pulsed wave Doppler mode. These modes allow the distinction between the left carotid artery

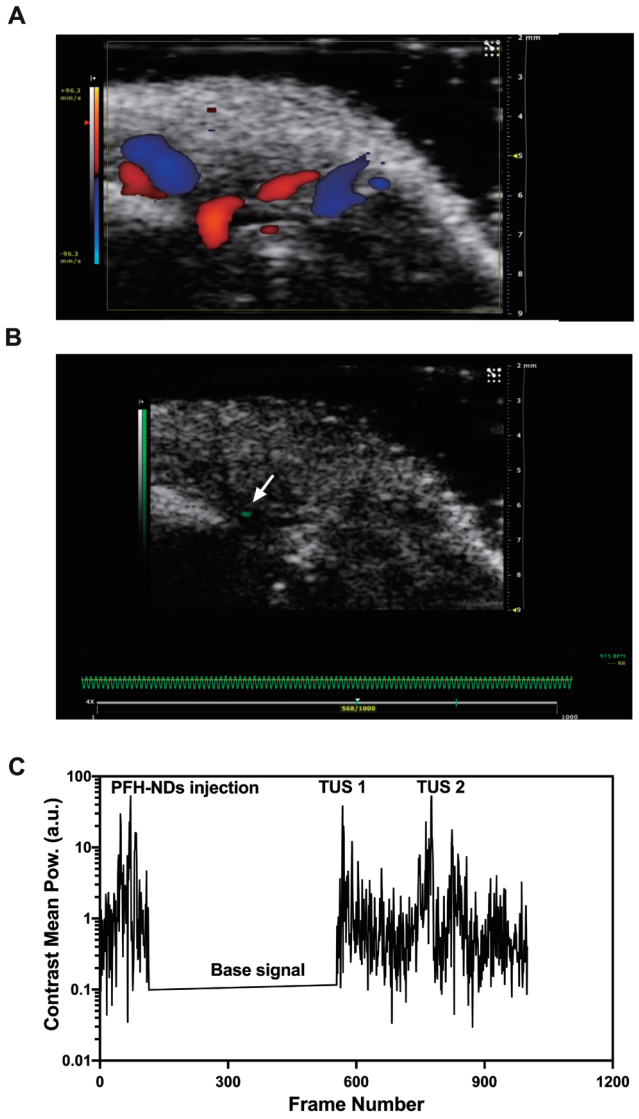

Fig. 5. *In Vivo* Ultrasonography of PFH-NDs in the Carotid Artery of Mice

(A) Doppler mode of carotid artery location. (B) The contrast enhancement signal of PFH-NDs after ultrasound irradiation. The arrow indicates the location of the bubbles in the carotid artery. (C) The overall contrast enhancement signal after repeated ultrasound irradiation. PFH-NDs containing 0.7% (v/v) PFH and 225 μg lipids were injected intravenously to mice *via* the tail vein. Upon confirming its location in advance with the Doppler mode, the region around the left carotid was imaged. During the monitoring period, two shots of ultrasound irradiation were applied to provoke phase transition of the droplets into bubbles.

and left internal jugular veins through the difference in the direction of the blood flow. Based on the anatomy of the region, the former and latter have been determined to be the carotid artery and jugular vein, respectively (Fig. 5A). Thus, the pulsed wave velocity at a pinpoint of the carotid artery region confirms the location and blood flow. In this experiment, the PFH-NDs were intravenously administered in a single dose, and ultrasonography imaging was initiated two minutes post-administration. After the first therapeutic ultrasound irradiation, contrast enhancement was noticed in the carotid artery region (Fig. 5B). Second ultrasound irradiation led to a repeated contrast enhancement that was sustained for a few hundred frames and ultimately decreased to the background levels (Fig. 5C).

DISCUSSION

PFH-NDs have been used as an ultrasound contrast agent or even as ultrasound-responsive carriers loaded with therapeutic drugs for their delivery.[22–24] Although theranostic functions of the NDs were investigated partially in them, the *in vivo* theranostic behaviour of PFH-NDs following systemic administration has remained unclear. In this study, we examined the theranostic potential of PFH-NDs under both the *in vitro* and *in vivo* conditions.

PFH-NDs prepared in this study had an average size of 205 ± 1.8 nm with relatively narrow size distribution. The use of zwitterionic phospholipid DSPC with a portion of DSPE-PEG_{2000} was effective for stabilizing PFH droplets. NR-PFH-NDs had a larger particle size of 346.3 ± 6 indicated that drug loading causes a slight increase in the particle size (Table 1). Moreover, the acoustic droplets vaporisation was achieved *in vitro* with therapeutic ultrasound irradiation in a frequency of 1 MHz rather than 3 MHz. As clearly shown in Fig. 2B, ultrasound signal was increased with increasing the intensity of ultrasound irradiation in a frequency of 1 MHz. We could not observe a similar result when ultrasound in 3 MHz was used, as shown in Fig. 2A, and it was indicated that PFH-NDs could only be activated with low-frequency ultrasound irradiation. The mechanical index (MI) value is an indication for the aggressiveness of ultrasound waves toward ultrasound contrast agents. In our simulation, MI value significantly increased in a low frequency of ultrasound irradiation; therefore, 1 MHz seems to provide sufficient forces for inducing the liquid-gas phase transition. Presumably, we could observe more clear contrast enhancement in ultrasound irradiation frequency of 1 MHz rather than 3 MHz as shown in Fig. 2C. Then we investigated the therapeutic aspect of PFH-NDs by loading the particles with NR as a hydrophobic drug model. NR can quickly be localized into cell membrane upon its release from PFH-NDs. NR uptake in C26 cells was enhanced when NR-PFH-NDs combined with ultrasound irradiation in a frequency of 1 MHz rather than in frequency of 2 MHz at the affixed intensity of 5 W/cm^2. The association of this result and *in vitro* phase transition observation shown in Fig. 2B suggests that ultrasound in a frequency of 1 MHz can induce the proper theranostic functions consisting of the high contrast signal and the efficient drug release from PFH-NDs shown in Fig. 3C. Concerning *in vivo* performance of PFH-NDs, we first evaluated PFH leakage from PFH-NDs during incubation at 37°C in the presence of serum. Serum components are reported to be the main factors that destabilize phospholipid based carriers such as liposomes.[25] In our study, PFH was almost retained in droplets for 90 min in the presence of rat serum. This result indicated that PFH-NDs could be well tolerated under *in vivo* conditions. In accordance with this finding, the GC-MS analysis showed that PFH-NDs could sustain PFH in the blood circulation of mice for a considerable long time after the intravenous injection. The PFH elimination half-life time of 43.3 min is much longer than those reported for ultrasound contrast agents made with gaseous or liquid perfluoropentane.[9,26] Thus, unlike microbubbles, our result indicated the benefit of the utilization of liquid pefluorehexane as well as to the incorporation of polyethylene glycol engraftment into droplets for producing stable nano-scaled theranostic ultrasound contrast agents. As shown in Fig. 5, the imaging

potential of PFH-NDs was confirmed by ultrasonography imaging in mice carotid artery, which revealed a high contrast enhancement signal at the carotid artery area after ultrasound irradiation. In addition, we showed that the contrast signal could repeatedly be generated by ultrasound irradiation (Fig. 5C). A future study of PFH-NDs for the delivery of nucleic acid drugs or anti-cancer agents would expand their utilities toward further theranostic applications.

CONCLUSION

In this study, we have evaluated the potential of PFH-NDs for theranostic purposes. The finding of *in vitro* acoustic droplets vaporization suggested that PFH-NDs were selectively triggered with ultrasound irradiation in the frequency of 1 MHz. The combination of NR-PFH-NDs and ultrasound irradiation in the frequency of 1 MHz also induced the localization of NR in mice C26 cells. After intravenous injection of PFH-NDs, PFH could be sustained in the blood circulation of mice and PFH-NDs were acoustically vaporized in the carotid artery by ultrasound irradiation with reproducible contrast signal. These results added valuable information on the potential of PFH-NDs as theranostic carriers mainly for systemic administration and on their rational design.

Acknowledgments This work was supported in part by JSPS KAKENHI under Grant numbers 23240072 (MH) and 16H01861 (MH), by the Programs for Promotion of Fundamental Studies in Health Sciences of the National Institute of Biomedical Innovation (MH) and by the Ministry of Education, Culture, Sports, Science and Technology (MEXT) of Japan. The author would like to thank Professor Shigeru Kawakami (Graduate School of Biomedical Sciences, Nagasaki University, Nagasaki, Japan), Associate Professor Ryo Suzuki (Faculty of Pharma-Sciences, Teikyo University, Tokyo, Japan) and Lecturer Yuriko Higuchi (Graduate School of Pharmaceutical Sciences, Kyoto University, Kyoto, Japan) for their kind advice and assistance during this research.

Conflict of Interest The authors declare no conflict of interest.

REFERENCES

1) Sirsi SR, Borden MA. State-of-the-art materials for ultrasound-triggered drug delivery. *Adv. Drug Deliv. Rev.*, **72**, 3–14 (2014).
2) Cai WB, Yang HL, Zhang J, Yin JK, Yang YL, Yuan LJ, Zhang L, Duan YY. The optimized fabrication of nanobubbles as ultrasound contrast agents for tumor imaging. *Sci. Rep.*, **5**, 13725 (2015).
3) Abdalkader R, Kawakami S, Unga J, Suzuki R, Maruyama K, Yamashita F, Hashida M. Evaluation of the potential of doxorubicin loaded microbubbles as a theranostic modality using a murine tumor model. *Acta Biomater.*, **19**, 112–118 (2015).
4) Stride E, Edirisinghe M. Novel microbubble preparation technologies. *Soft Matter*, **4**, 2350–2359 (2008).
5) Qin S, Caskey CF, Ferrara KW. Ultrasound contrast microbubbles in imaging and therapy: physical principles and engineering. *Phys. Med. Biol.*, **54**, R27–R57 (2009).
6) Abdalkader R, Kawakami S, Unga J, Higuchi Y, Suzuki R, Maruyama K, Yamashita F, Hashida M. The development of mechanically formed stable nanobubbles intended for sonoporation-mediated gene transfection. *Drug Deliv.*, **24**, 320–327 (2017).
7) Tinkov S, Winter G, Coester C, Bekeredjian R. New doxorubicin-loaded phospholipid microbubbles for targeted tumor therapy: Part I—Formulation development and *in-vitro* characterization. *J. Control. Release*, **143**, 143–150 (2010).
8) Escoffre J-M, Mannaris C, Geers B, Novell A, Lentacker I, Averkiou M, Bouakaz A. Doxorubicin liposome-loaded microbubbles for contrast imaging and ultrasound-triggered drug delivery. *IEEE Trans. Ultrason. Ferroelectr. Freq. Control*, **60**, 78–87 (2013).
9) Toft KG, Hustvedt SO, Hals PA, Oulie I, Uran S, Landmark K, Normann PT, Skotland T. Disposition of perfluorobutane in rats after intravenous injection of Sonazoid™. *Ultrasound Med. Biol.*, **32**, 107–114 (2006).
10) Kwan JJ, Borden MA. Lipid monolayer collapse and microbubble stability. *Adv. Colloid Interface Sci.*, **183–184**, 82–99 (2012).
11) Chen CC, Sheeran PS, Wu S-Y, Olumolade OO, Dayton PA, Konofagou EE. Targeted drug delivery with focused ultrasound-induced blood-brain barrier opening using acoustically-activated nanodroplets. *J. Control. Release*, **172**, 795–804 (2013).
12) Rapoport N, Nam KH, Gupta R, Gao Z, Mohan P, Payne A, Todd N, Liu X, Kim T, Shea J, Scaife C, Parker DL, Jeong EK, Kennedy AM. Ultrasound-mediated tumor imaging and nanotherapy using drug loaded, block copolymer stabilized perfluorocarbon nanoemulsions. *J. Control. Release*, **153**, 4–15 (2011).
13) Borden MA, Kruse DE, Caskey CF, Zhao S, Dayton PA, Ferrara KW. Influence of lipid shell physicochemical properties on ultrasound-induced microbubble destruction. *IEEE Trans. Ultrason. Ferroelectr. Freq. Control*, **52**, 1992–2002 (2005).
14) Kawabata K-I, Sugita N, Yoshikawa H, Azuma T, Umemura S-I. Nanoparticles with multiple perfluorocarbons for controllable ultrasonically induced phase shifting. *Jpn. J. Appl. Phys.*, **44** (6B), 4548–4552 (2005).
15) Sheeran PS, Dayton PA. Improving the performance of phase-change perfluorocarbon droplets for medical ultrasonography: current progress, challenges, and prospects. *Scientifica*, **2014**, 57968 (2014).
16) Ishijima A, Tanaka J, Azuma T, Minamihata K, Yamaguchi S, Kobayashi E, Nagamune T, Sakuma I. The lifetime evaluation of vapourised phase-change nano-droplets. *Ultrasonics*, **69**, 97–105 (2016).
17) Lanza GM, Winter PM, Caruthers SD, Hughes MS, Hu G, Schmieder AH, Wickline SA. Theragnostics for tumor and plaque angiogenesis with perfluorocarbon nanoemulsions. *Angiogenesis*, **13**, 189–202 (2010).
18) Cheng Y, Cheng H, Jiang C, Qiu X, Wang K, Huan W, Yuan A, Wu J, Hu Y. Perfluorocarbon nanoparticles enhance reactive oxygen levels and tumour growth inhibition in photodynamic therapy. *Nat. Commun.*, **6**, 8785 (2015).
19) Chen W-T, Kang S-T, Lin J-L, Wang C-H, Chen R-C, Yeh C-K. Targeted tumor theranostics using folate-conjugated and camptothecin-loaded acoustic nanodroplets in a mouse xenograft model. *Biomaterials*, **53**, 699–708 (2015).
20) Vlaisavljevich E, Durmaz YY, Maxwell A, ElSayed M, Xu Z. Nanodroplet-mediated histotripsy for image-guided targeted ultrasound cell ablation. *Theranostics*, **3**, 851–864 (2013).
21) Oda Y, Suzuki R, Mori T, Takahashi H, Natsugari H, Omata D, Unga J, Uruga H, Sugii M, Kawakami S, Higuchi Y, Yamashita F, Hashida M, Maruyama K. Development of fluorous lipid-based nanobubbles for efficiently containing perfluoropropane. *Int. J. Pharm.*, **487**, 64–71 (2015).
22) Kornmann LM, Curfs DMJ, Hermeling E, van der Made I, de Winther MP, Reneman RS, Reesink KD, Hoeks AP. Perfluorohexane-loaded macrophages as a novel ultrasound contrast agent: A feasibility study. *Mol. Imaging Biol.*, **10**, 264–270 (2008).
23) Simons JMM, Kornmann LM, Reesink KD, Hoeks APG, Kemmere MF, Meuldijk J, Keurentjes JTF. Monodisperse perfluorohexane emulsions for targeted ultrasound contrast imaging. *J. Mater.*

Chem., **20**, 3918 (2010).
24) Hannah AS, Luke GP, Emelianov SY. Blinking phase-change nanocapsules enable background-free ultrasound imaging. *Theranostics*, **6**, 1866–1876 (2016).
25) Allen TM, Cleland LG. Serum-induced leakage of liposome contents. *BBA-Biomembr*., **597**, 418–426 (1980).
26) Shiraishi K, Endoh R, Furuhata H, Nishihara M, Suzuki R, Maruyama K, Oda Y, Jo J, Tabata Y, Yamamoto J, Yokoyama M. A facile preparation method of a PFC-containing nano-sized emulsion for theranostics of solid tumors. *Int. J. Pharm*., **421**, 379–387 (2011).